Journal of Applied Polymer Science

Effect of strain level on stress relaxation and recovery behaviors of isotactic biaxially oriented polypropylene films

Altan Bozdoğan,[1] Baki Aksakal,[1] Kenan Koç,[1] Ekaterina Sergeevna Tsobkallo[2]

[1]Department of Physics, Yildiz Technical University, Esenler Istanbul, Turkey

[2]Department of Mechanics of Materials, St. Petersburg State University of Technology and Design, St. Petersburg, Russia

Correspondence to: A. Bozdoğan (E-mail: abozdog@yildiz.edu.tr)

ABSTRACT: The long-term recovery process and the changes in the uniaxial tensile properties and in the structure of isotactic biaxially oriented polypropylene (i-boPP) films after pre-extended at strain levels ranging from 1% up to 130% at room conditions were examined by using tensile testing, Fourier transform infrared spectroscopy/attenuated total reflectance, atomic force microscopy, and X-ray diffraction methods. It is significantly observed that the pre-extended i-boPP films at strain levels from 1% to 6% recovered completely back to their initial lengths and tensile properties. However, the i-boPP films showed a very slow recovery process and obtained very high remaining deformations changing with time which indicates irreversible structural processes after they were extended at higher strain levels. In order to predict the remaining deformation or length and the characteristics of the recovery process at any time, the linear equation of strain with respect to log time was proposed. The reasons for the changes in the tensile properties, the morphology, and the structure of the pre-extended i-boPP films were examined in detail. © 2015 Wiley Periodicals, Inc. J. Appl. Polym. Sci. **2016**, *133*, 42948.

KEYWORDS: degradation; mechanical properties; morphology; properties and characterization; X-ray

Received 3 July 2015; accepted 16 September 2015

DOI: 10.1002/app.42948

INTRODUCTION

Polypropylene (PP) is one of the most widely used polymers for the production of different materials and has various produced forms such as PP films, filaments, sutures, and yarns. In order to improve the properties of PP film, which has greater applications in industry and daily life[1] than those in other forms, such as mechanical properties (tensile strength and Young's modulus), optical (haze, gloss) and barrier properties, biaxial orientation which means that stretching is applied in both directions, i.e., the machine direction (MD) and the transverse direction (TD), is seen to be a well-known method in production processes.[2,3] Among the oriented PP films, the biaxially oriented polypropylene (boPP) film is used in a variety of applications such as packaging for biscuits, crisps, baked goods, sweets; cigarette wrap, shrink wrap; industrial films and due to being less expensive it has replaced more expensive packing materials.[3–5] A well-known type of boPP film, that is, isotactic biaxially oriented polypropylene (i-boPP) film is greatly produced and the world production of this material is quite high and about 2 million tons per year.[5] When compared with other commonly used polymers, the isotactic boPP film has a range of remarkable properties such as good water barrier properties,[1] good elastic properties under short-time action, low specific density (~0.92 g/cm^3), high chemical resistance, almost zero hygroscopicity, and good dielectric properties.[5]

From the structural point of view, isotactic polypropylene (i-PP) can be divided into α, β, and γ phases. α-iPP phase is the most common crystalline form. Their density and melting temperature are 0.94 g/cm^3 and 180°C, respectively. The α_1 and α_2 forms have monoclinic C2/c and P2$_1$/c symmetries, respectively.

It is clear that during the working life of i-boPP products, these kinds of products are exposed to various external effects such as stress, extension, and temperature. Thus, the structural units, that is, amorphous phase and crystalline regions, (lamellae) undergo the mechanical and thermal deformation and destruction processes which result mainly in the breakage of the polymer chains. During mechanical treatments, the i-boPP films show relaxation: creep, stress relaxation, and elastic recovery and such processes result in noticeable inhomogeneous changes in the deformation of amorphous regions which is located between lamellae and linked to the lamellae by tie molecules and chain entanglements and the radially oriented lamellae.[6] The response of the material to straining at a constant speed, that is, the tensile deformation or behavior, is characterized by using the stress–strain curve of i-boPP films which is generally divided into elastic and plastic deformation. The elastic deformation is generally attributed to the small recoverable changes in bond angles and length of the molecules in the structure. On the other hand, the plastic deformation is seen at larger strain

values after the yield point and the difference of the plastic deformation between amorphous and crystalline regions becomes more distinctive. In general, the elastic property of the polymer materials is a very important characteristic and the residual component of deformation of the polymer materials after being extended or stretched at different strain levels is very important because residual deformation may lead to undesirable property of the materials in use. Thus, the examination of the accumulation of the residual deformation which comes out after generally stress-relaxation and creep processes in time is very important for the materials in practice.

In the literature, the stress-relaxation behaviors of PP at different forms such as thin films, PP-based composites, fibers, and sutures at different temperatures and the effect of stress-relaxation processes on their deformation properties were discussed in some studies[6–13] and some studies were devoted to propose and discuss the mathematical description of the stress-relaxation process and viscoelasticity and viscoplasticity of isotactic PP.[4,11,14] Influence of stretching and drawing on the surface and structure of the PP films were discussed in some studies which involved generally the effect of the stretching conditions in the production stages of boPP films.[15–18] However, except few studies[19,20] which dealt with the effect of the level of preliminary deformation on the stiffness of the oriented PP fibers there is not any detailed study investigating the effect of preliminary extensions following stress relaxation on the uniaxial tensile properties of boPP films and the strain recovery process in long time.

Thus, our study aimed to investigate the influence of the preliminary extensions up to around 130% strain following short-term stress-relaxation process of i-boPP films on the uniaxial tensile properties such as Young's modulus, tensile strength, and breaking extension determined by stress–strain curves and the recovery process of applied strain on the stretched i-boPP films in long time up to around 1.5 years. Mechanical, morphological, and structural changes were examined by using the tensile testing, Fourier transform infrared spectroscopy (FT-IR), atomic force microscopy (AFM), X-ray diffraction (XRD) methods in detailed. The changes in the structure and tensile properties were discussed and the equations for the prediction of the strain recovery process in long term were proposed, which enable one to estimate the residual deformations due to plastic deformations at any time in the process.

MATERIALS AND EXPERIMENTAL

Materials

In the experiments, i-boPP films were provided from Polinas (Istanbul, Turkey). The films have the thickness of 30 μm. For different kind of experiments, the films were cut into strips with different widths and several cm in length.

Methods

Methods for Tensile Testing Measurements and Stress-Relaxation and Recovery Process. Uniaxial tensile tests and stress-relaxation tests of i-boPP films were investigated on a Lloyd tensile testing machine LF Plus (AMETEK Lloyd Inst., UK) with a crosshead speed of 20 mm/min at room conditions (T = 20°C; RH = 65%). The films with thickness of 30 μm and width of 1 mm were used in the tensile tests and stress-relaxation experiments. The gauge length of the tested i-boPP films was chosen to be 20 mm. Before measurements, the test film was stuck carefully in a paper frame.

The stress–strain curves of the unstretched and stretched samples were obtained at the same constant strain rate of 100%/min (20 mm/min) at 20°C and a relative humidity of 65%.

The stress-relaxation experiments were carried out with the same method explained earlier[21]: in the first step, the sample was stretched up to an adjusted deformation level (ε_{pe}). In the second step, the sample was held for 10 min in its stretched form during which the strain was kept constant and the stress relaxation process occurred. As soon as the film sample was relieved from that strain level, the residual length (strain) on the sample was measured in the same equipment for the recovery times up to around 10 min. Then, for longer recovery times, the residual deformations were investigated by measuring the length of the sample in that position in time with a vernier.

The stress–strain curve of the stretched i-boPP films were recorded after approximately 5 min following the stress relaxation of 10 min by considering new cross-section of the stretched sample with the same gauge length. The stress values of the sample in stress-relaxation experiments were calculated using the initial cross-sectional area of the sample.

The stress relaxation, strain recovery processes, and the stress–strain curves of i-boPP films after being stretched at a wide extension range from 0 to approximately 130% strain were obtained, and their mechanical characteristics were investigated.

Spectroscopic Measurements. Infrared experiments were carried out on a PerkinElmer Fourier Transform Spectrometer "Spectrum One" (PerkinElmer, USA) utilizing an attenuated total reflectance (ATR) cell. In order to investigate the structural changes after stretching i-boPP films, the i-boPP films with width of 5 mm and a suitable initial length to the stretching equipment were stretched in a rectangular handmade metal frame which enables us to stretch the sample at desired strain ratio. FT-IR–ATR spectra of the stretched film samples were recorded in the 650–4000 cm^{-1} range at a resolution of 4 cm^{-1} with four scans for each measurement.

Method for AFM Measurements. Surface morphologies of the samples were investigated by an atomic force microscope (AFM, SPM-9500J3, Shimadzu) operating in the dynamic mode. The AFM images of i-boPP thin films which were stretched at different strain levels were recorded at stretched states of the samples.

Method for XRD Measurements. XRD measurements were performed on a diffractometer (XRD, GBC-MMA) operated at 35 kV and 28 mA using CuKα radiation at room temperature. The XRD patterns were scanned in the 2θ range 10–30°. The XRD pattern of the stretched i-boPP films at different strain levels from 0% to 110% were obtained at stretched states of the samples.

RESULTS AND DISCUSSION

The Effect of Strain History on Tensile Properties of i-boPP Films at Room Conditions

The i-boPP films obtained stretched form which shows different stress strain curves as seen in Figure 1 and different tensile characteristics as

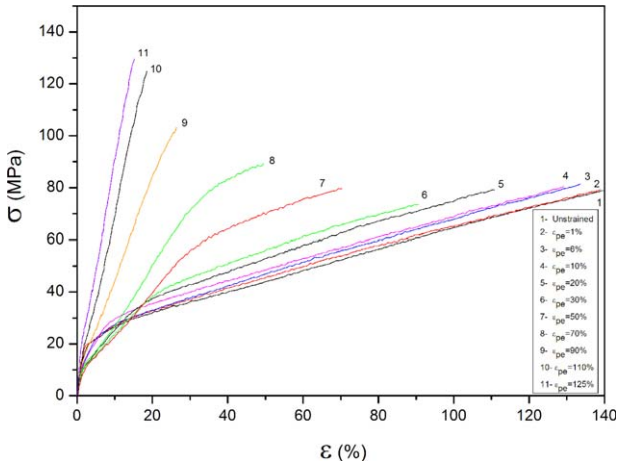

Figure 1. The stress–strain curves of i-boPP films after the application of different strain levels (ε_{pe}) at room conditions. [Color figure can be viewed in the online issue, which is available at wileyonlinelibrary.com.]

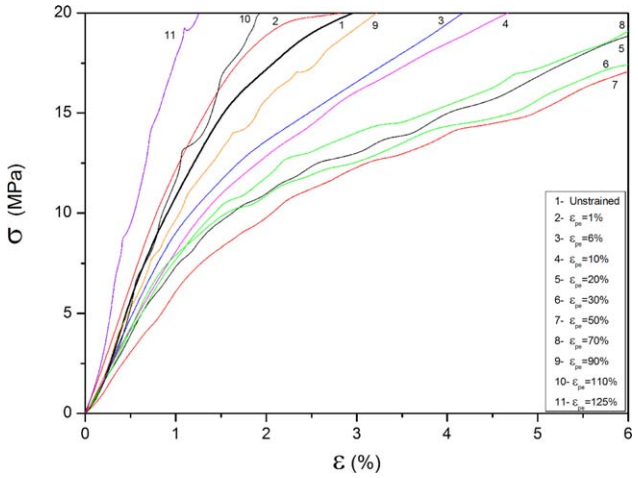

Figure 2. The change of initial part of the stress–strain curves of i-boPP films with respect to applied strain at different levels. [Color figure can be viewed in the online issue, which is available at wileyonlinelibrary.com.]

tabulated in Table I, as a result of the short-time stress relaxation which results strain history at different levels.

In general, a typical stress–strain curve of oriented PP films can be characterized with two deformational regions.[22–26] The first region ranging up to around 2% strain corresponds to elastic and reversible small deformations. Beyond yield point, second deformation region from approximately 8–10% to the breakage point occurs which corresponds to plastic deformation, that is, irreversible process of molecular ordering and orientation of amorphous segments and crystalline regions together with some chain breakages.

As seen in Figure 1, after the application of low preliminary extension levels (ε_{pe}) ranging from 0% to 10%, the shape of stress–strain curve became the same as unstrained film. Here, while the breaking extension (ε_r) decreases slightly, tensile strength (σ_r) became almost the same as that of unstrained sample. For ε_{pe} being greater than 10% and less than approximately 90%, the stretched i-obPP films obtained different stress–strain curve caused by more rigid structure. As it is seen in Table I, although σ_r increases little, ε_r decreases dramatically. It is noticed that the stress–strain curve shows another turning point shifting from around 18% to 35%. We assume that the chain breakage in amorphous regions of oriented structure accelerated. For higher strain than 80%, because the structural elements, i.e., crystalline regions and amorphous chains were much oriented and stressed. The highly stretched films do not elongate much and that is why it breaks at very low extension and very high stress values.

Table I. The Tensile Characteristics of i-boPP Films Strained at Different Levels

ε_{pe} (%)	E_{young} (GPa)	ε_r (%)	σ_r (MPa)	U_T (J m^{-3} 10^4)
0	1.39	140.01	78.80	7232.28
1	1.34	138.83	79.37	7273.24
6	1.06	133.58	81.44	7091.13
10	1.02	129.15	80.54	6908.81
20	0.9	110.79	79.13	5895.84
30	0.83	90.62	73.55	4561.82
50	0.62	70.24	79.60	3736.31
70	0.82	49.44	89.37	2755.52
90	1.06	26.37	103.09	1500.86
110	1.41	18.54	124.83	1212.46
125	2.05	15.28	129.59	1075.80

As it is seen in Table I, with increasing ε_{pe} up to around 50%, Young's modulus (E_y) decreased from around 1.4 to 0.6 GPa and then, it increased up to around 2 GPa. The changes in E_y value and in the initial part of the stress–strain curve with increasing ε_{pe} levels are apparently shown in Figures 2 and 3. Moreover, the toughness (U_T) of the i-obPP films decreased first slowly for ε_{pe} up to 10% strain and then decreased greatly. We assume that the pre-extension level up to around 4% results in almost reversible process caused by small changes in bond angles and lengths, and in intermolecular interactions such as Van der Waals forces. Thus, initial modules become close to that of unstrained sample.

We know that stretching leads to predominantly orientation process of the structural units. For the pre-extension levels from around 6% to 50%, we think that firstly, entanglements in amorphous chains are opened and the amorphous chains are aligned in stretching direction. During the orientation process, some chain breakage comes out in especially amorphous chains as explained in FT-IR/ATR spectral analysis part. Hence, a significant decrease is seen in Young's modulus (Figures 2 and 3).

On the other hand, during the molecular ordering in the amorphous regions and process of chain orientation at higher strain levels (>50%), the zones of parallel arrangement of macromolecules in a rigid form which causes obstacle for chain scissions were produced. In partially ordered domains, more uniform stress is distributed over individual chain and mobility of macromolecular segments is restricted. Because these effects are more dominant than the process of bond breakages in especially

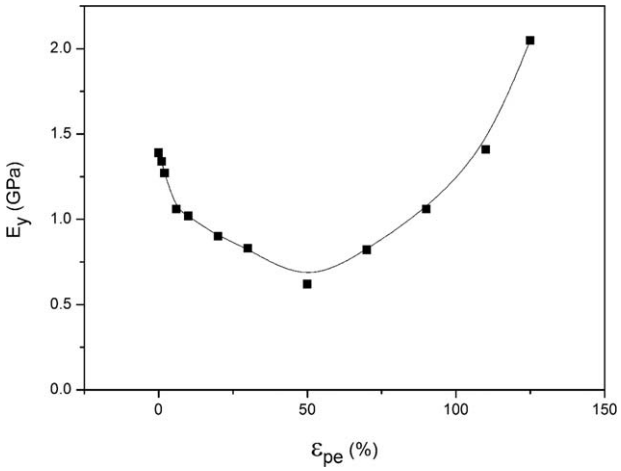

Figure 3. The changes in Young's modulus of i-boPP films with respect to applied strain at different levels.

amorphous regions,[5,27] Young's modulus increased greatly as seen in Figures 2 and 3.

Short-Time Stress-Relaxation and following Long-Term Recovery Process of i-boPP Films at Wide Range of Strain Levels

The stress-relaxation curves of i-boPP films at wide range of strain levels during 10 min are given in Figure 4. In general, during the stress-relaxation process, the load in the sample decreases fast in the first stage and then continues slowly with time.

As explained in study of Deng and Zhou,[28] generally the stress relaxation process can be characterized by three stress-relaxation regions: fast (1); slow (2) stress-relaxation region; and transition region (3) between these two regions. The fast stress-relaxation region corresponds to mostly elastic deformation and ends quickly. In the slow stress-relaxation region which forms the most stress-relaxation process, the specimen responds to the applied strain viscoelastically and the stress in the specimen decreases gradually. Due to high viscoelastic deformation occurring in this region, the specimen obtains a residual deformation

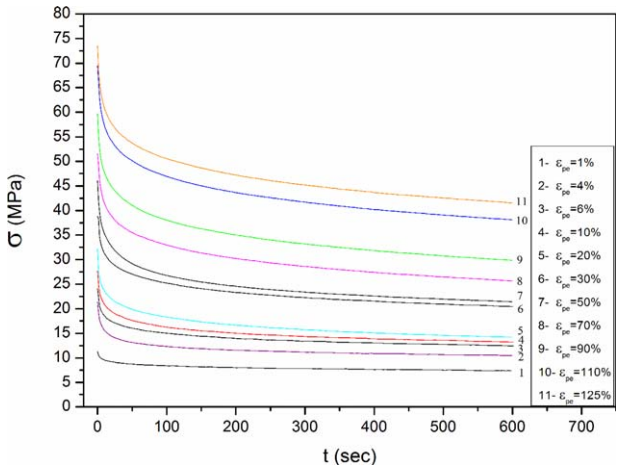

Figure 4. The stress-relaxation behaviours of i-boPP films with respect to applied strain at different levels. [Color figure can be viewed in the online issue, which is available at wileyonlinelibrary.com.]

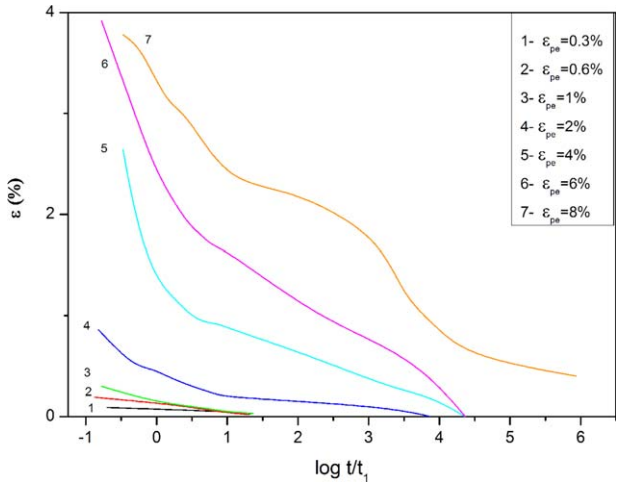

Figure 5. The recovery curves in strained i-boPP films at different preliminary strain (ε_{pe}) levels from 0.3% to 8% in the ε-log t coordinates. [Color figure can be viewed in the online issue, which is available at wileyonlinelibrary.com.]

(length) depending on time after the end of stress-relaxation experiment. According to authors (Deng and·Zhou), transition region is completed in a few minutes.

As seen in Figure 4, the fast stress-relaxation occurs in the initial part of the stress-relaxation curves that is up to 5 s of relaxation time. The transition region ranges from 5 to approximately 100 s depending on applied stress levels. After this transition region, the slow stress-relaxation process occurs and results in residual deformation which increases with increasing stress levels.

After the stress-relaxation process, the strained sample released from the stretched position. The residual deformation (ε_{Res}) that is the residual length on the stretched film was measured during long term (~600 days). The recovery of the deformation was depicted in the ε-log t coordinates as shown in Figures 5 and 6. It is seen that the preliminary extension levels up to around 6% did not cause big structural changes and deformations. It resulted in almost recoverable deformation in the structure. Hence, we see that the strained films in this region recovered back completely to the original length. That is why we observed very similar stress–strain curve to that of unstrained i-boPP film.

However, as shown in Figure 6, with increasing ε_{pe} levels, the residual deformation increases greatly. We know that while the stress level or ε_{pe} level increase, as a result of molecular rearrangement, stretching, and orientation process of structural units, the bond breakages in the especially amorphous regions increase. Although some part of the deformation can be elastic and recoverable, the most of the deformation is viscoelastic and irreversible. As it is noticed some part of the deformation is recovered in time; however, because the recovery process is very slow, the sample has a big residual deformation even after 600 days (more than 1.5 years) at room condition.

The very slow recovery process is also seen in Figure 7. Here, it is seen that as strain levels increase up to around 40%, the residual deformation is become very low and increased very slowly. Beyond 40% strain, the residual deformation increases

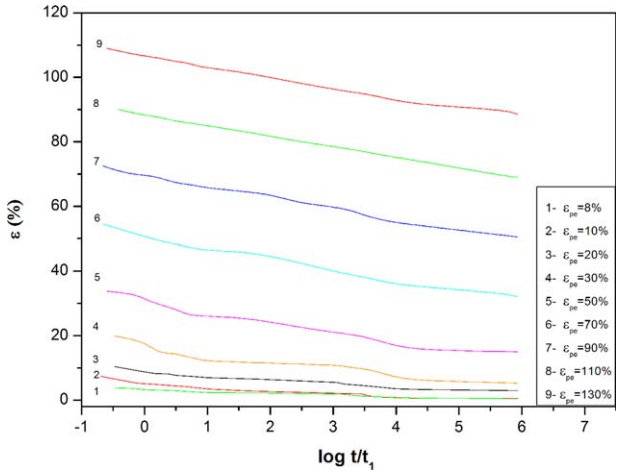

Figure 6. The family of recovery curves in strained i-boPP films at different preliminary strain (ε_{pe}) levels from 8% to 130% in the ε-log t coordinates. [Color figure can be viewed in the online issue, which is available at wileyonlinelibrary.com.]

almost linearly with increasing strain level. However, it is common for each strain level higher than approximately 8%, the recovery process is very slow. For instance, if the applied strain level value equaling 90% is considered, after 10 min recovery the ε_{res} is about 73% of the original applied 90% deformation; after 1 day recovery ε_{res} becomes 66% of the applied strain and after 600 days it became around 56% of the applied strain.

By using the dependencies shown in Figure 6, we have the possibility to estimate the remaining deformations in stretched i-boPP films at any strain levels in the wide time range. By considering a linear approach for each curve, we can calculate the approximate value of residual deformation by the following equation;

$$\varepsilon(t) = \varepsilon_i - A_i \log(t/t_1) \quad (1)$$

where ε_i is the strain value of i-boPP films when the time equals one minute and A_i is the slope value of the each curve which

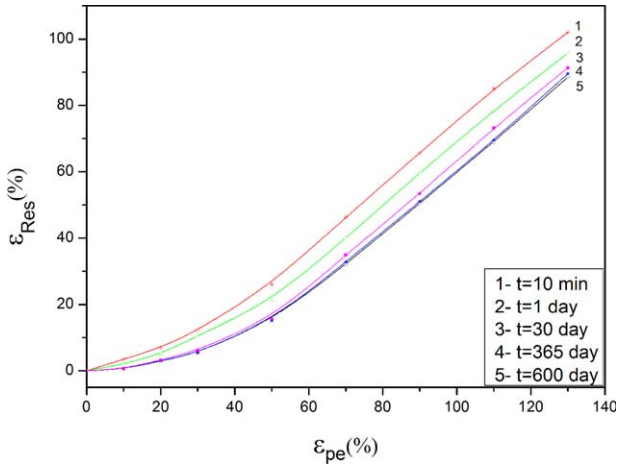

Figure 7. The change of remaining deformation (ε_{Res}) from different applied strain levels (ε_{pe}) after different recovery times. [Color figure can be viewed in the online issue, which is available at wileyonlinelibrary.com.]

Table II. The Parameters of the Linear Curves for Characterizing the Recovery Properties of Stretched i-boPP Films

ε_{pe} (%)	ε_i (%)	A_i (%)	R^2
8	3.27	0.55	0.95
10	5.14	0.99	0.89
20	8.56	1.13	0.94
30	15.92	1.98	0.87
50	30.24	3.03	0.94
70	50.52	3.31	0.98
90	69.44	3.37	0.99
110	88.32	3.28	1.00
130	106.39	3.14	0.99

was calculated by using linear curve fitting and listed in Table II. Here, t_1 is a constant equaling 1 min chosen for the unit consistency.

As it is seen in Table II, the parameter A_i considered as the velocity of the recovery process increases with increasing strain level up to 90% and then it decreased slightly. However, it is clear that we have to wait for very long time for a stretched i-boPP films recover back completely to its initial form and structure at room condition.

FT-IR/ATR Spectral Results

The FT-IR/ATR spectra of pre-extended i-boPP films are seen in Figure 8. The significant changes are seen in the range of 950–1030 and 1600–1800 cm^{-1}, which give the information about the changes of isotacticity or crystallinity and degradation products, respectively.

We know that as a result of applied stress (strain), UV light, γ irradiation, plasma treatment, electrical field, etc., degradation in PP films come out. These effects generally cause β-scission, peroxide, and hydroperoxides radicals.[29] Some chemical species containing hydroxyl (OH) groups, carbonyl (C═O) groups, and unsaturated (C═C) groups are formed. That is, some degradation products such as alcohol, carboxylic acids, ketones, aldehydes, esters, and γ-lactones can be formed.[24] In the spectra shown in Figure 8, multiple overlapping carbonyl peaks appear at around 1720–1735 cm^{-1}. These bands were assigned to the groups of carboxylic of esters and aldehyde or ketone.[29] Here, the band at 1711 or 1715 cm^{-1} is attributed to the carbonyl groups of ketone.[29] The band observed at around 1735 cm^{-1} belongs to the oxygen-containing terminal groups.[5] In the range of 1400–1800 cm^{-1}, the band originating from double C═C bond[29] referred to the terminal (—CH═CH_2) position of the diene groups[5,30] was observed at around 1640 cm^{-1} which was seen as a clearly separated band in some pre-extension levels and as an overlapping band in some other pre-extension levels like the case for the bands observed at 1711 and 1735 cm^{-1} in the spectra.

In order to see the changes in the absorbance intensities of the bands observed at 1711–1715, 1640, and 1735 cm^{-1}, the relative absorbance intensities of each band to that of the methylene group observed at around 1456 cm^{-1} was calculated by using

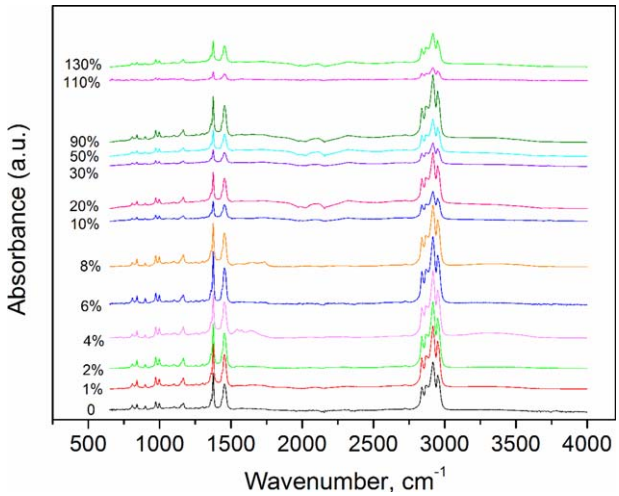

Figure 8. FT-IR/ATR spectra of i-boPP films being pre-extended at different strain levels. [Color figure can be viewed in the online issue, which is available at wileyonlinelibrary.com.]

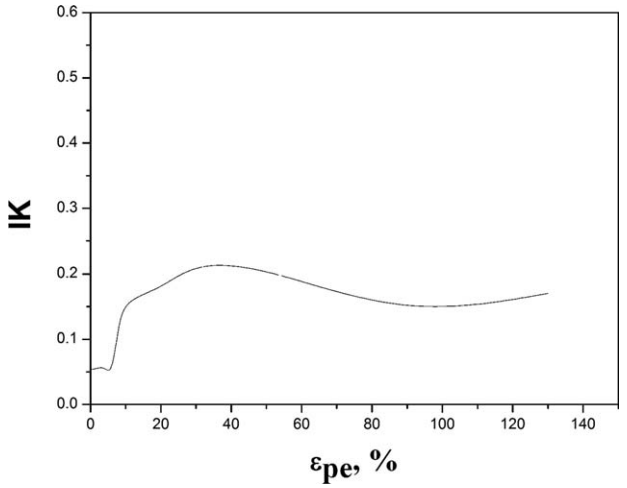

Figure 9. The change of ketone carbonyl index (IK) with increasing preliminary extension levels (ε_{pe}).

flat baselines drawn from 1505 ± 3 to 1975 ± 3 cm^{-1} for the bands observed 1711–1715, 1640, and 1735 cm^{-1} and from 1402 ± 2 to 1504 ± 2 cm^{-1} for the peak at 1456 cm^{-1}. The absorbance intensity of the methylene group bending was used as standard band, because it was supposedly unchanged and independent on the destruction process.[5,29] Here, the relative absorbance intensity of the ketone group corresponding to 1711 or 1715 cm^{-1} to that of standard band is known as ketone carbonyl index (IK) and calculated by the following equation.

$$\text{Ketone carbonyl index IK} = \frac{A_{1711}}{A_{1456}} \text{ or } \frac{A_{1715}}{A_{1456}} \quad (2)$$

Moreover, in order to determine the changes in isotacticity (helical regularity) or crystallinity of i-obPP, the isotacticity (ISO) was calculated by the relative absorbance intensity of the bands observed at 998 and 973 cm^{-1},[1,29,31,32] by using the flat base lines drawn from 925 to 1018 ± 3 cm^{-1}.

$$\text{Isotacticity (ISO)} = \left(\frac{A_{998}}{A_{973}}\right) \times 100 \quad (3)$$

As a result of analysis of the IK and other degradation products containing carbonyl groups observed at around 1735 cm^{-1}, it was observed that the changing tendency of the former is very similar to that of the latter with increasing preliminary extension levels. As an example, the changes of IK in stretched i-boPP films at different strain levels is given in Figure 9. Here, it is seen that at low strain values up to around 4%, IK became almost constant and very close to zero. This shows that almost no significant degradation resulting in chain breaking came out. However, after preliminary extension of 6–8% strain, the IK increased noticeably which shows the increase in the Ketone groups and significant chain breakages. Furthermore, IK became maximum for the extension levels at around 40% strain. Then, it did not change much and can be supposed nearly constant with increasing extension levels.

The changes in the relative absorbance intensity of the band 1640 cm^{-1} to that of standard band is given in Figure 10. Similar changing tendency is seen with increasing strain levels. That is, for low strain values up to around 4–6%, the absorbance ratio is very small and constant which shows the deformation is very small and these strain values do not cause significant structural changes resulting in the chain breakages. However, after strain levels of 8–10%, a noticeable change in the absorbance ratio is obtained and this ratio gets nearly maximal values for strain levels around 50%, after which the ratio can be considered constant or change very little. We suppose that these diene groups considered as oxygen-free "defect" groups started to increase remarkably after strain levels of 8–10% and increasing strain levels did not increase the concentration of these groups significantly.

On the other hand, the change of isotacticity with increasing strain levels is given in Table III.

Here, it is seen as a general tendency with increasing preliminary extension levels, the isotacticity or regularity related with the crystallinity decreased slightly. This shows that crystalline and regular regions did not damage much with increasing deformation levels. Even at very high extension level of 130%,

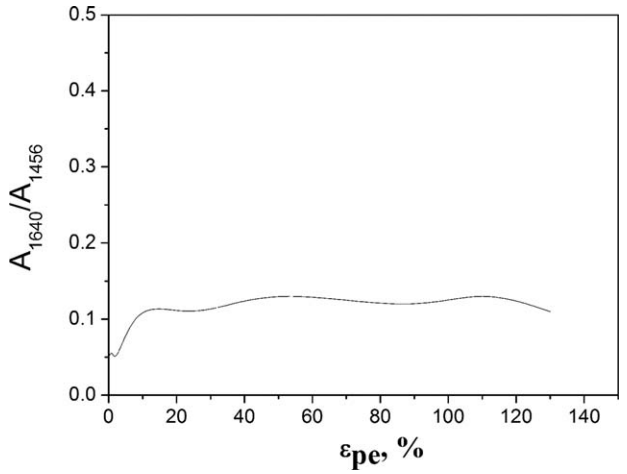

Figure 10. The change of relative absorbance ratio of the oxygen-free "defect" band to internal standard band for different preliminary extension levels (ε_{pe}).

Table III. Isotacticity of the Strained i-boPP Films at Different Preliminary Extension Levels (ε_{pe})

ε_{pe} (%)	ISO (%)
0	77.21
6	76.07
20	75.82
50	74.38
90	73.69
130	70.0

the decrease in the isotacticity is about 9%. Consequently, this result leads us to suppose that the chain breakages and degradation products take place mostly in amorphous regions.

AFM and XRD Results

The AFM images (scanning area 5 μm × 5 μm) of PP films at different strain level are given in Figure 11. As seen in Table IV, while the stress level or ε_{pe} level increase, the maximum *z*-range and root mean square (RMS) roughness values of the surface increase for i-boPP film. As the maximum z-range and RMS values were 39 nm and 5.3 nm for unstretched i-boPP film, these values increased up to 163 nm and 14.3 nm for ε_{pe} = 110%, respectively. The i-boPP films consist of amorphous and crystalline structures. In case of unstretched state, the structures that are close to each other (amorphous and crystalline structures) constitute more firm and as a consequence also a smoother film surface. This tight and well-ordered structure has been opened by stretching. Consequently, the film surface becomes more intricate. Hence, the maximum *z*-range and RMS values have been increased.

The main reason for this is the amorphous regions that connect the crystallites each other are opened more than the crystal

Table IV. The Maximum *z*-Range and RMS Values of i-boPP for Different sStrain Levels

	0%	10%	30%	70%	110%
Maximum *z*-range (nm)	39	61	97	115	163
RMS (nm)	5.3	6.5	8.8	12.6	14.3

region. These two structures (amorphous and crystalline) that cannot be opened at the same rate led to the conclusion that initially more tight and smooth surface became more intricate and rougher as stretched level increased.

The XRD spectra of pre-extended i-boPP films are seen in Figure 12. The XRD patterns exhibits prominent broad peaks at 2θ values of 14.11°, 16.96°, 18.67° and d-spacing values (nm) are 0.627, 0.522, and 0.475 for unstrained material (ε_{pe} = 0%). These peaks are in agreement with (110), (040), and (130) reflection planes, respectively, and show alpha crystalline phase indexed as α-PP.[24,33] The average crystallite sizes can be calculated from the XRD patterns using the Scherrer's formula given below:

$$t_{hkl} = \frac{0.9\lambda}{\beta \cos\theta}$$

where λ is the wavelength of X-ray (0.154 nm), β is the full width at half maximum (FWHM), θ is the angle of diffraction (in rad). $t_{hkl}$is the crystallite size (in nm) along the direction perpendicular to the crystallographic plane *hkl*. The average crystallite sizes of i-boPP films were calculated using the peaks corresponding to (110) and (040) planes, and the obtained results are given in Table V. As seen in Table V, the crystallite sizes of i-boPP films decreased with the increasing strain levels

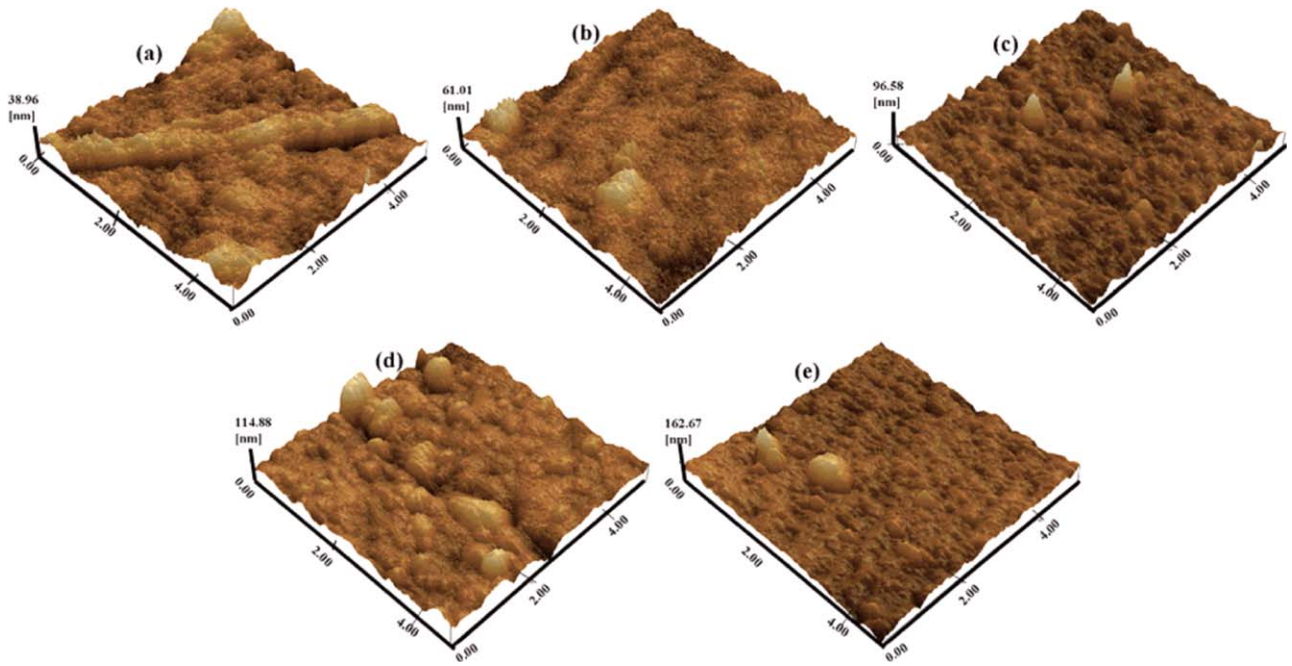

Figure 11. AFM images of the stretched i-boPP films at (a) ε = 0%, (b) ε = 10%, (c) ε = 30%, (d) ε = 70%, and (e) ε = 110%. [Color figure can be viewed in the online issue, which is available at wileyonlinelibrary.com.]

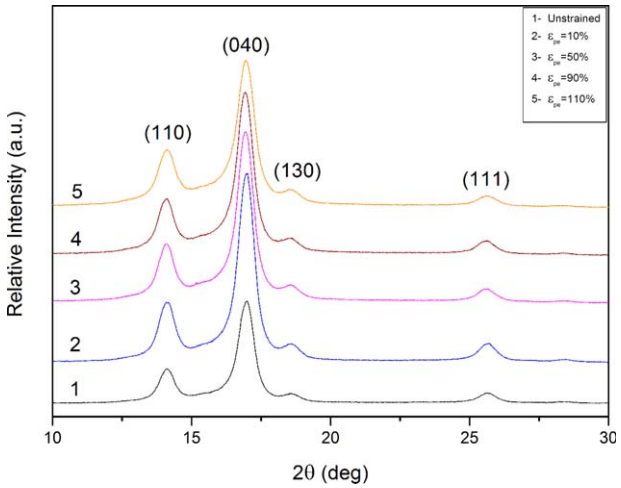

Figure 12. XRD spectra of pre-extended i-boPP films at various strain levels. [Color figure can be viewed in the online issue, which is available at wileyonlinelibrary.com.]

while interplanar distances (d) were almost the same. These results explain the slightly decrease in isotacticity and the increase in roughness of i-boPP films while stretching obtained FT-IR/ATR and AFM results, respectively. Namely, the results of isotacticity show that crystalline regions did not damage much with increasing deformation levels. On the other hand, the XRD results show that the crystallite size did not change significantly and so the crystalline domains remained almost intact as the ε_{pe} level increases. Therefore, the amorphous regions were opened more than the crystal region and the maximum z-range and RMS values increased as the ε_{pe} level increases. Moreover, it is usually known that if half-width of the XRD peak is large, it corresponds to smaller crystallites. Hence, the broaden peaks in the XRD patterns clearly indicates that the nanosize crystallite behavior of the i-boPP films. Contribution to broadening can also be due to lattice distortion and structural disorder.

CONCLUSIONS

The results of tensile tests of pre-extended i-obPP films at different strain levels from 1% up to very high 125% showed that Young's modulus decreased from around 1.4 GPa to 0.6 GPa as ε_{pe} level increased up to 50% and the modulus significantly increased up to around 2 GPa. While the i-obPP film can obtain increasing tensile strength value, its extensibility decreased slowly for ε_{pe} values up to 10% and then decreased dramatically which show that the pre-extended i-obPP films became stronger but more brittle, that is why the toughness of the material decreased greatly for ε_{pe} higher than 10% strain.

Table V. 2θ and Crystallite Size Values of (110) and (440) Planes for Different Strain Levels

	2θ (deg)		Crystallite size, t_{hkl} (nm)	
ε_{pe} (%)	(110)	(440)	(110)	(440)
0	14.11	16.96	11.927	12.231
10	14.11	16.96	11.352	12.027
50	14.09	16.92	10.965	11.768
90	14.09	16.91	10.638	11.672
110	14.12	16.94	9.528	10.697

From the results of the stress-relaxation and long-term recovery processes, it was clearly observed that pre-extended i-oPP films recovered completely back to initial length for low ε_{pe} values up to 6% strain. However, for higher ε_{pe} levels, the i-oPP films showed irreversible structural process, thus, they obtained very slow recovery process in which the residual deformations increased significantly. Besides, a linear function of strain with respect to log (t/t_1) was introduced to predict the long-term behavior of the recovery process and the remaining deformations at any time.

The FT-IR/ATR measurements revealed that with increasing ε_{pe} level the isotacticity related with the crystallinity decreased slightly which indicates the crystalline domains did not degrade significantly. This tendency is also seen in the change in the crystallite size which did not decrease much as shown in the XRD analysis. As a consequence of AFM results, it can be seen that as the ε_{pe} level increases, the maximum z-range and RMS values increased. This shows that although the film surface initially became tight and well-ordered in unstretched form, it became more intricate and rougher caused by the fact that amorphous regions can be able to be opened and aligned faster that the crystalline region.

It is concluded that pre-extended i-oPP films recovered completely back to initial length for low ε_{pe} values (up to 6%) and its residual deformation reached a saturation after long-term creep process. These results are useful and should be considered for the prediction of the behavior of oriented PP materials undergoing preliminary extensions at different strain level in the daily use or industrial applications.

ACKNOWLEDGMENTS

The authors would like to thank Prof. Dr. Fatma Tepehan for her laboratory facilities.

REFERENCES

1. Calafut, T. In Plastic Films in Food Packaging, PDL Handbook Series; Ebnesajjad, S., Ed.; Elsevier: New York, **2012**; Chapter 6, p 93.
2. Briston, J. H.; Katan, L. L. Plastic Films; Longman Scientific and Technical: Harlow, **1989**.
3. Breil, J. In Plastic Films in Food Packaging, PDL Handbook Series; Ebnesajjad, S., Ed.; Elsevier: New York, **2012**; Chapter 4, p 53.
4. Tsobkallo, E. S.; Tikhomirov, A. A.; Balanev, A. S.; Petrova, L. N. *Fibre Chem.* **2008**, *40*, 381.
5. Tsobkallo, K.; Tikhomirov, A; Bozdogan, A.; Tshemel, A. *J. Appl. Polym. Sci.* **2006**, *102*, 6074.
6. Tscharnuter, D.; Jerabek, M.; Major, Z.; Pinter, G. *Eur. Polym. J.* **2011**, *47*, 989.

7. Kinay, A. E.; Brostow, W.; Castano, V. M.; Maksimov, R.; Olszynski, P. *Polymer* **2002**, *43*, 3593.
8. Deng, M.; Zhou, J. *J. Mater. Sci. Mater. Med.* **2006**, *17*, 365.
9. Razavi-Nouri, M. *Iran J. Chem. Chem. Eng.* **2012**, *9*, 60.
10. Sweeney, J.; O'Connor, C. P. J.; Spencer, P. E.; Pua, H.; Caton-Rose, P.; Martin, P. *J. Mech. Mater.* **2012**, *54*, 55.
11. Drozdov, A. D. *Eng. Fract. Mech.* **2010**, *77*, 2277.
12. Andreassen, E. *Polymer* **1999**, *40*, 3909.
13. Tsobkallo, E. S.; Chmel, A. E.; Tikhomirov, A. A. *Fibre Chem.* **2006**, *38*, 41.
14. Drozdov, A. D.; Gupta, R. K. *Int. J. Eng. Sci.* **2003**, *41*, 2335.
15. Ran, S.; Xu, M. *Chinese J. Polym. Sci.* **2004**, *22*, 123.
16. Kerddonfag, N.; Saravari, O.; Chinsirikul, W. *Adv. Mater.* **2011**, *239242*, 1939.
17. Fujiyama, M.; Kawamura, Y.; Wakino, T.; Okamoto, T. *J. Appl. Polym. Sci.* **1988**, *36*, 995.
18. Díez, F. J.; Alvariño, C.; López, J.; Ramírez, C.; Abad, M. J.; Cano, J.; García-Garabal, S.; Barral, L. *J. Therm. Anal. Calorim.* **2005**, *81*, 21.
19. Tsobkallo, E. S.; Tiranov, V. G.; Gromova, E. S. *Fibre Chem.* **2001**, *33*, 215.
20. Tsobkallo, E. S.; Nachinkin, O. I.; Kvartskheliya, V. A. *Fibre Chem.* **1998**, *30*, 168.
21. Tsobkallo, K.; Aksakal, B.; Darvish, D. *J. Appl. Polym. Sci.* **2012**, *125*, E168.
22. Ward, I. M.; Sweeney, J. An Introduction to the Mechanical Properties of Solid Polymers; Wiley: West Sussex, **2004**; p 53.
23. Bower, D. I. An Introduction to Polymer Physics; Cambridge University Press: New York; **2002**; p 162.
24. Karger-Kocsis, J. Polypropylene: An A–Z Reference; Kluver: Dordrecht, **1999**; Vol. 1–3, p 233–239, 607–614, 891–895.
25. Maier, C.; Calafut, T. Polypropylene: The Definitive User's Guide and Databook; Plastics Design Library: Norwich, NY; **1998**; p 11.
26. Karian, H. G. Handbook of Polypropylene and Polypropylene Composites; Marcel Dekker Inc.: New York, **2003**; p 25.
27. Incarnato, L.; Scarfato, P.; Acierno, D. *Polym. Eng. Sci.* **1999**, *39*, 749.
28. Deng, M.; Zhou, J. *J. Mater. Sci. Mater. Med.* **2006**, *17*, 365.
29. Longo, C.; Savaris, M.; Zeni, M.; Brandalise, R. N.; Grisa, A. M. C. *Mater. Res.* **2011**, *14*, 442.
30. Dechant, J. Ultratspektroskopische Untersuchungen an Polymeren; Akademischer Verlag: Berlin, **1972**.
31. Ren, W. *Colloid. Polym. Sci.* **1992**, *270*, 747.
32. Zaiqing, W.; Xingzhou, H.; Deyan, S. *Chinese J. Polym. Sci.* **1988**, *6*, 285.
33. Mukhopadhyay, N.; Panwar, A. S.; Kumar, G.; Samajdar, I.; Bhattacharyya, A. R. *Phys. Chem. Chem. Phys.* **2015**, *17*, 4293.